THE JOURNAL OF BIOLOGICAL CHEMISTRY VOL. 290, NO. 2, pp. 1269–1280, January 9, 2015

Negative Regulation of Melanoma Differentiation-associated Gene 5 (MDA5)-dependent Antiviral Innate Immune Responses by Arf-like Protein 5B*

Received for publication, September 13, 2014, and in revised form, November 14, 2014 Published, JBC Papers in Press, December 1, 2014, DOI 10.1074/jbc.M114.611053

Yuichi Kitai[‡§¶], Osamu Takeuchi[‖], Takumi Kawasaki[‡], Daisuke Ori[‖], Takuya Sueyoshi[‡], Motoya Murase[‡], Shizuo Akira[§¶], and Taro Kawai[‡1]

From the [‡]Laboratory of Molecular Immunobiology, Graduate School of Biological Sciences, Nara Institute of Science and Technology (NAIST), 8916-5 Takayama-cho, Ikoma, Nara 630-0192, Japan, the [§]Laboratory of Host Defense, Immunology Frontier Research Center (IFReC) and [¶]Department of Host Defense, Research Institute for Microbial Diseases, Osaka University, 3-1 Yamada-oka, Suita, Osaka 565-0871, Japan, and the [‖]Laboratory of Infection and Prevention, Institute for Virus Research, Kyoto University, 53 Shogoin Kawara-cho, Sakyo-ku, Kyoto 606-8507, Japan

Backgrounds: Melanoma differentiation-associated gene 5 (MDA5)-mediated signaling contributes to antiviral innate immunity.
Results: Overexpression of ADP-ribosylation factor-like protein 5B (Arl5B) repressed the MDA5-induced activation of the interferon β promoter. Arl5B-deficient cells showed up-regulation of MDA5-mediated responses.
Conclusion: Arl5B is a negative regulator of MDA5 signaling.
Significance: Arl5B is an important suppressor for antiviral innate immune response.

RIG-I-like receptors (RLRs), including retinoic acid-inducible gene-I (RIG-I) and MDA5, constitute a family of cytoplasmic RNA helicases that senses viral RNA and mounts antiviral innate immunity by producing type I interferons and inflammatory cytokines. Despite their essential roles in antiviral host defense, RLR signaling is negatively regulated to protect the host from excessive inflammation and autoimmunity. Here, we identified ADP-ribosylation factor-like protein 5B (Arl5B), an Arl family small GTPase, as a regulator of RLR signaling through MDA5 but not RIG-I. Overexpression of Arl5B repressed interferon β promoter activation by MDA5 but not RIG-I, and its knockdown enhanced MDA5-mediated responses. Furthermore, Arl5B-deficient mouse embryonic fibroblast cells exhibited increased type I interferon expression in response to MDA5 agonists such as poly(I:C) and encephalomyocarditis virus. Arl5B-mediated negative regulation of MDA5 signaling does not require its GTP binding ability but requires Arl5B binding to the C-terminal domain of MDA5, which prevents interaction between MDA5 and poly(I:C). Our results, therefore, suggest that Arl5B is a negative regulator for MDA5.

The retinoic acid-inducible gene-I (RIG-I)[2]-like receptors (RLRs), melanoma differentiation-associated gene 5 (MDA5), and LGP2 play central roles in triggering innate immune responses against RNA virus infection by recognizing viral RNA in the cytoplasm (1, 2). RIG-I and MDA5 possess an N-terminal region composed of tandem caspase recruitment domains (CARDs) that mediate downstream signaling, a central DExD/H-box helicase/ATPase domain, and a C-terminal domain (CTD) that is responsible for RNA recognition. LGP2 lacks the N-terminal CARDs and acts as a regulator of RIG-I and MDA5 signaling. RIG-I and MDA5 differentially recognize viral RNA. RIG-I preferentially recognizes short double-stranded (ds) RNA containing 5′-triphosphates. RIG-I is required for antiviral responses against Newcastle disease virus (NDV), vesicular stomatitis virus, influenza A viruses, measles virus, and Ebola virus. In contrast, MDA5 recognizes long dsRNA and the synthetic dsRNA analog polyinosinic:polycytidylic acid (poly(I:C)) and is activated by encephalomyocarditis virus (EMCV) (2).

In response to virus infection, RIG-I and MDA5 initiate signaling cascades that lead to activation of the transcription factor interferon regulatory factor 3 (IRF3) and nuclear factor κB (NFκB), which control transcription of target genes encoding type I interferon (IFN) and inflammatory cytokines. In the absence of viral RNA, RIG-I masks its CARDs by the CTD, but RNA recognition induces conformational changes of RIG-I that enable the CARDs to interact with a mitochondria-localized CARD-containing adaptor IPS-1 (also known as MAVS/Cardif/VISA) (2–4). RIG-I activation involves protein modifications such as ubiquitination, and TRIM25, RNF135 (Riplet or REUL), and MEX3C are E3 ubiquitin ligases that enhance RIG-I signaling by K63 polyubiquitination (5–8). In contrast, MDA5 forms filaments along with dsRNA that are required for association with IPS-1 (9–11). The interaction between RIG-I/MDA5 and IPS-1 induces prion-like aggregates of IPS-1 on the mitochondrial membrane to propagate antiviral signaling pathways (12). IPS-1 then interacts with TRAF3, resulting in the

* This work was supported by a KAKENHI Grant-in-aid for Scientific Research (B) 26293107 and by the Japan Society for the Promotion of Science through the Funding Program for World-Leading Innovative R&D on Science and Technology (FIRST Program), The Cell Science Research Foundation, and The Naito Foundation.
[1] To whom correspondence should be addressed. Tel.: 81-743-72-5550; Fax: 81-743-72-5559; E-mail: tarokawai@bs.naist.jp.
[2] The abbreviations used are: RIG-I, retinoic acid-inducible gene-I; RLR, RIG-I-like receptor; MDA5, melanoma differentiation-associated gene 5; Arl5B, ADP-ribosylation factor-like protein 5B; CARD, caspase recruitment domains; CTD, C-terminal domain; dsRNA, double-stranded; NDV, Newcastle disease virus; EMCV, encephalomyocarditis virus; IRF3, interferon regulatory factor 3; Arl, ADP-ribosylation factor-like protein; MS, multiple sclerosis; MEF, mouse embryonic fibroblast; qPCR, quantitative PCR.

activation of a kinase complex involving TBK1 and IKKi, which mediate phosphorylation of IRF3. Simultaneously, IPS-1 interacts with TRAF6 and activates the IKK complex consisting of IKKα, IKKβ, and NEMO, which phosphorylates IκBs. Phosphorylated IκBs are degraded, enabling the transcription factor NFκB to translocate into the nucleus for subsequent induction of genes encoding inflammatory cytokines (4, 13, 14).

Although MDA5 and RIG-I play essential roles in eliciting antiviral immune responses, their aberrant activation results in the development of autoimmune and inflammatory diseases if they engage with host endogenous RNA or if their signaling pathways become constitutively active. Single nucleotide polymorphisms of RIG-I and MDA5 are reported to correlate with systemic lupus erythematosus and multiple sclerosis (MS) (15, 16). It has been shown recently that RNA degradation products generated during the unfolded protein response are a source of endogenous RLR agonists, and this response was inhibited by the cytosolic exosomes, which are produced by SKIV2L RNA helicases (17). A recent study showed that a gain-of-function mutant of MDA5 developed lupus-like nephritis in a murine model (18). Furthermore, numerous molecules that inhibit MDA5 and RIG-I signaling have been identified. A20, NLRX1, gC1qR, Arl16, and DAK bind to RLRs or IPS-1 to inhibit antiviral responses (19–23). RNF125 inhibits RIG-I signaling by K48 polyubiquitination and proteasome-mediated degradation of RIG-I (24). CYLD and USP4 are deubiquitinases that remove K63- or K48-linked polyubiquitin chains, respectively, from RIG-I to inhibit RIG-I signaling (25, 26). Collectively, there are multiple mechanisms that negatively regulate RLR-mediated antiviral responses.

Members of the ADP-ribosylation factor-like protein (Arl) family are low molecular weight guanine-nucleotide-binding proteins that control membrane trafficking and organelle structure (27). Their functions are regulated through a cycle of GTP binding (active form) and GTP hydrolysis (inactive from) involving guanine nucleotide exchange factor and GTPase activating protein. There are >20 Arl genes in mouse and human, and several of them participate in the regulation of immune responses. For instance, Arl16 negatively regulates RIG-I-mediated signaling by interacting with the C-terminal repressor domain of RIG-I (21). Arl8B is required for the polarization of lytic granules toward the immune synapse in natural killer cells and their cytotoxicity (28).

Here, we identified Arl5B as a negative regulator of MDA5 signaling. Arl5B has been shown to be an IFNβ-inducible gene and to be highly expressed in the peripheral blood cells of MS patients (29). Our study shows that Arl5B negatively regulates MDA5-mediated signaling by interfering with MDA5-dsRNA binding and illustrates the importance of Arl5B in regulating antiviral innate immunity.

EXPERIMENTAL PROCEDURES

Reagents, Cells, and Viruses—LPS, short poly(I:C), poly(I:C), and puromycin were purchased from InvivoGen. G418 was purchased from Nacalai Tesque. All cells were cultured in Dulbecco's modified Eagle's medium (Nacalai Tesque) supplemented with 10% fetal bovine serum (Invitrogen) and 0.05 mM 2-mercaptoethanol (Nacalai Tesque) at 37 °C in a humidified 5% CO_2, 95% air atmosphere. Mouse embryonic fibroblasts (MEFs) were obtained from pregnant mice at embryonic day 9.5 according to a previous paper (30). EMCVs and NDVs were prepared as described previously (30).

Plasmid Construction—Expression plasmids for the Arl family members were constructed by PCR using cDNA from murine macrophages, brain, liver, and embryonic fibroblasts as a template. The resulting PCR products were inserted into pcDNA3 that contained an Myc-tag sequence. Expression plasmids for Arl5B D1, D2, D3, and D4 were prepared by PCR mutagenesis using pcDNA3-Arl5B-Myc as a template. IFNβ and NFκB promoter luciferase reporters and expression plasmids for MDA5, IPS-1, TRIF, IRF3, TBK-1, and RIG-I were described previously (30).

Generation of Arl5B Heterogenic Mice—The Arl5B gene was isolated from genomic DNA extracted from ES cells (GSI-I) by PCR. The targeting plasmid was constructed by replacing a 2-kb fragment encoding the Arl5B open reading frame (exons 2 and 3) with a neomycin-resistance gene cassette (Neo^r), and a herpes simplex virus thymidine kinase (TK) driven by the phosphoglycerate kinase (PGK) promoter was inserted into the genomic fragment for negative selection. After the targeting plasmid was transfected into ES cells, G418 and ganciclovir double-resistant colonies were selected and screened by PCR and further confirmed by Southern blot analysis. Homologous recombinants were microinjected into C57BL/6 female mice, and heterozygous F1 progenies were backcrossed with C57BL/6 >5 generations. All animal experiments were performed with the approval of the Animal Research Committee of the Research Institute for Microbial Diseases, Osaka University, and the Nara Institute of Science and Technology.

Southern Blotting—The genomic DNA was extracted from Arl5B heterogenic ES cells and digested with BamHI. The digested DNA was loaded to agarose gel electrophoresis and transferred to a nylon membrane. The membrane was hybridized with denatured labeled probe, washed, and visualized with autoradiography. The probe DNA of Arl5B genomic locus was amplified from the genomic DNA of ES cells by PCR using a pair of following primers: 5′-acagggtaaatggcccttagtagctggc-3′ and 5′-ctttcttcacagcatagggaactctggc-3′.

Genotyping for Arl5B-deficient MEFs—Genotyping was carried by PCR using the extracted DNA from MEFs and the following primer sets: Arl5B_common (5′-gcaagaaaagagttctctctccgtgaagc-3′) and Arl5B_wild (5′-gtctggctctgttaaacaacgccaaagc-3′) or PGK-RC2 (5′-ctaaagcgcatgctccagactgccttg-3′). Arl5B_common and Arl5B_wild primers were used to detect wild type allele, and Arl5B_common and PGK-RC2 primers were used to detect mutated allele.

Luciferase Assay—HEK293 cells were cultured in 24-well plates semi-confluently and transfected with 100 ng of pFLAG6c-hMDA5, 500 ng of pcDNA3-Arl5B-Myc, 10 ng of pRL-TK (Promega), and 30 ng of pGL3-IFNβ promoter or pNFκB-Luc by using Lipofectamine 2000 (Invitrogen). After 48 h from the transfection, the cells were lysed and subjected to a luciferase assay using a dual-luciferase reporter assay system (Promega) according to the manufacturer's instructions.

Knockdown—For the construction of shRNA-expressing retroviral vectors, the oligo DNA was inserted into the BglII and

TABLE 1
Primer sequences for qPCR analysis

Primer	Sequence
18S_rRNA_forward	gtaacccgttgaaccccatt
18S_rRNA_reverse	ccatccaatcggtagtagcg
Arl5b_forward	gcccatgaggatttaaggaa
Arl5b_reverse	gggtggtccttgattgaact
Ifna_forward	tctgatgcagcaggtggg
Ifna_reverse	agggctctccagacttctgctctg
Ifnb1_forward	cagctccaagaaaggacgaac
Ifnb1_reverse	ggcagtgtaactcttctgcat
Il6_forward	tccagttgccttcttgggac
Il6_reverse	gtactccagaagaccagagg
Tnf_forward	tccccaaagggatgagaagtt
Tnf_reverse	gtttgctacgacgtgggctac

HindIII sites of pSUPER.retro.puro (OligoEngine). The oligo DNA sequence was indicated as below; Scramble shRNA, 5′-cctaaggctatgaagagatacttcaagagagtatctcttcatagccttattttt-3′; Arl5B shRNA#1, 5′-ccggctgatcttcgctaaactgtggttcaagagaccacagtttagcgaagatcagccttttt-3′; Arl5B shRNA#2, 5′-ccaccataggaagcaatgttgaagattcaagagatcttcaacattgcttcctatggtttttt-3′; Arl5B shRNA#3, 5′-cccagcattcaagtagatgttgtgcttcaagagagcacaacatctacttgaatgctgtttttt-3′. The retroviral vectors were transfected into Plat-E cells by using Lipofectamine 2000. The virus was filtered with a 0.22-μm filter at 48 h post-transfection and infected into MEFs. Forty-eight hours after the infection MEFs were treated with 2 μg/ml puromycin for 48 h, and then knockdown efficiency was measured by RT-qPCR. Plat-E cells were kind gifts from T. Kitamura (The University of Tokyo, Tokyo, Japan).

Retroviral Expression of Arl5B in MEFs—Arl5B cDNA was inserted into BglII and EcoRI sites of pMSCVpuro (Clontech), and then the virus preparation and MEFs selection were performed as described above under "Knockdown."

qPCR—MEFs (1×10^5 cells) were seeded in each well of 6-well plates and cultured overnight. The cells were stimulated with LPS, short poly(I:C), or poly(I:C) for the indicated conditions, and then total RNA were isolated by using TRIzol (Invitrogen) according to the manufacturer's instructions. Stimulation with poly(I:C) and short poly(I:C) was carried out by transfection using Lipofectamine 2000. cDNA was synthesized from the isolated RNA by using ReverTra Ace (TOYOBO) with random hexamer primers according to the manufacturer's instructions. Semiquantitative analysis of mRNA levels was performed with a LightCycler 96 system (Roche Applied Science). Primer sets for qPCR analysis were described in Table 1.

Immunoprecipitation and Immunoblotting—HEK293T cells cultured in 60-mm dishes were transfected with 4 μg of Arl5B expression plasmids together with 2 μg of MDA5 or RIG-I expression plasmids by using Lipofectamine 2000. The cells were lysed in 20 mM Tris-HCl, pH 8.0, 150 mM NaCl, 1 mM EDTA, 0.5% Nonidet P-40, and the cell lysates were immunoprecipitated with 5 μl of anti-Myc antibody-conjugated agarose beads (c-Myc 9E10, sc-40 AC, Santa Cruz Biotechnology). The samples were applied to SDS-PAGE and then immunoblotted as described previously (8). The used antibodies were listed as below: anti-Myc rabbit antibody (×1000 dilution, Sigma); anti-FLAG rabbit antibody (×1000 dilution, Sigma), or anti-β-actin goat antibody (×1000 dilution, I-19, Santa Cruz Biotechnology).

ELISA—MEFs (2.0×10^4 cells) were seeded on 96-well plates and stimulated for 24 h with the indicated amounts of LPS, short poly(I:C), or poly(I:C). The cytokine levels in the culture supernatant were measured by using a mouse IL-6 Duoset and a Mouse CXCL10 Duoset (R&D Systems) according to the manufacture's instructions.

Immunofluorescence—HEK293T cells grown on 12-mm glass coverslips (Matsunami Glass) were transfected with 250 ng of pcDNA3-Arl5B-Myc and 250 ng of pFLAG6c-hMDA5 by using Lipofectamine 2000. In the case of MEFs, the cells were stimulated with 1 μg/ml poly(I:C) using Lipofectamine 2000 after growth on glass coverslips. The cells were fixed and stained with primary antibodies: anti-FLAG mouse antibody (×5000 dilution, M2; Sigma); anti-Myc rabbit antibody (×300 dilution; Sigma); anti-G3BP rabbit antibody (×200 dilution; Sigma); secondary antibodies Alexa Fluor 488 goat anti-mouse IgG antibody (×3000 dilution; Molecular Probes) and Alexa Fluor 594 goat anti-rabbit IgG antibody (×3000 dilution; Molecular Probes) together with 1 μg/ml Hoechst 33412 (Sigma). The cells on the coverslip were observed using a fluorescent microscope (BZ-9000, Keyence) and confocal microscope (FV1000, Olympus).

Immunoblotting for Arl5B, Phosphorylated-IRF3 and -NFκB p65—MEFs were cultured in 6-well plates semi-confluently and stimulated with the indicated amounts of LPS, short poly(I:C), or poly(I:C). Cells were then lysed in 50 mM Tris-HCl, pH 8.0, 150 mM NaCl, 1% Nonidet P-40, 0.5% sodium deoxycholate, and 0.1% SDS. For the detection of Arl5B, the cells were lysed in 50 mM Tris-HCl, pH 8.0, 150 mM NaCl, 1% Nonidet P-40, and then immunoprecipitated with 5 μl of anti-Arl5B rabbit antibody (Proteintech Group) and 20 μl of protein G-Sepharose 4 Fast Flow (GE healthcare) overnight at 4 °C. The samples were applied to SDS-PAGE and immunoblotted with anti-Arl5B (×300 dilution), anti-IRF3 (D83B9, Cell Signaling Technology), anti-phospho-IRF3 (Ser-396, 4D4G, Cell Signaling Technology), anti-NFκB p65 (D14E12, Cell Signaling Technology), or anti-phospho-NFκB p65 antibody (Ser-536, 93H1, Cell Signaling Technology).

Poly(I:C) Binding Assay—HEK293T cells transiently transfected with MDA5 and Arl5B expression plasmids by Lipofectamine 2000 were lysed in 400 μl of 20 mM Tris-HCl, pH 8.0, 150 mM NaCl, 1% Nonidet P-40, and 1 mM EDTA, and the cell lysates were precipitated with 40 μl of poly(I:C)-conjugated agarose beads for 2 h at 4 °C. The samples were washed and applied to SDS-PAGE, and then immunoblotted. Poly(I:C)-conjugated agarose beads were prepared as described previously (31).

NFκB Activation Assay—MEFs cultured in 100-mm dishes were stimulated with short poly(I:C) or poly(I:C). The cells were then lysed in 10 mM HEPES-KOH, pH 7.8, 11 mM KCl, 0.2 mM EDTA, 0.6% Nonidet P-40, and complete protease inhibitor mixture (Roche Applied Science). After centrifugation, the supernatants were discarded, and nuclear extracts were prepared by lysing the pellets in 20 mM HEPES-KOH, pH 7.8, 420 mM NaCl, 20% glycerol, 0.2 mM EDTA, 2 mM $MgCl_2$, and complete protease inhibitor mixture with vigorous shaking. DNA binding activity of NFκB in the nuclear extracts was measured using NF-κB p50/p65 transcription factor assay kit (Abcam) according to the manufacturer's instructions.

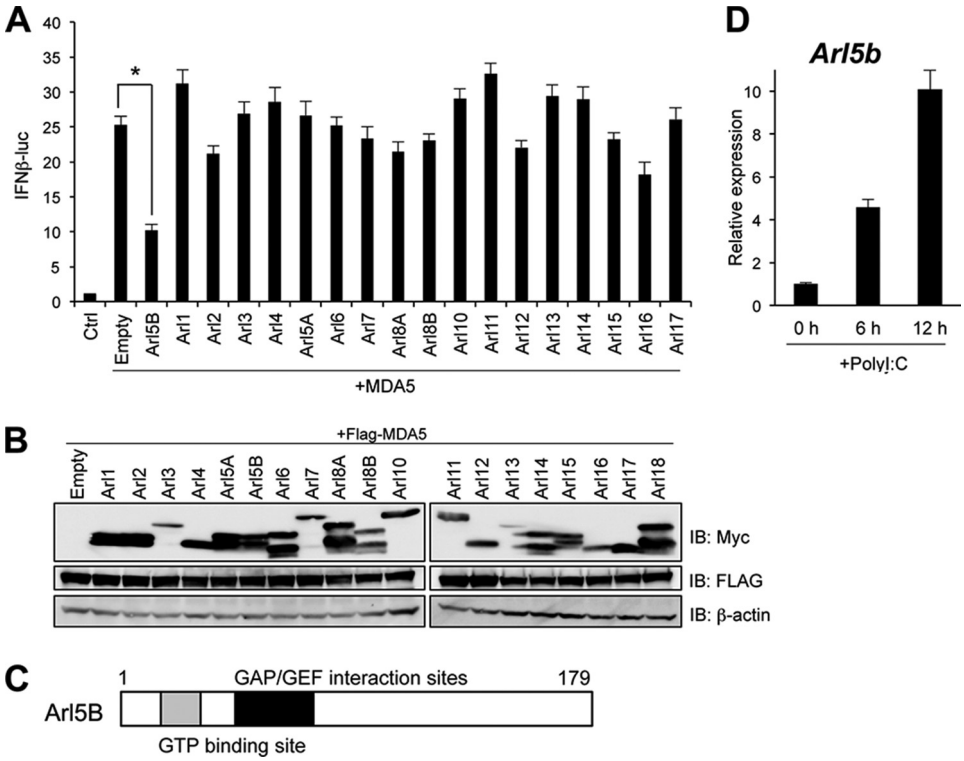

FIGURE 1. **Screening of Arl family members that regulate MDA5 signaling.** *A*, HEK293 cells were transiently cotransfected with expression plasmids for MDA5 and the indicated Arl family member together with an IFNβ promoter-driven luciferase reporter plasmid. Luciferase activity was measured at 48 h post-transfection ($n = 3$; mean values and S.E. are depicted). *B*, cell lysates prepared from HEK293 cells transiently transfected with the indicated plasmids were subjected to immunoblotting (*IB*) with the indicated antibodies. *C*, conserved domains of Arl5B. Arl5B is a small G protein possessing GTPase activating protein/guanine nucleotide exchange factor (*GAP/GEF*) interaction sites. *Numbers* represent amino acid positions. *D*, MEFs were stimulated with 1 μg/ml poly(I:C) for the indicated periods, and the expression of Arl5b was measured by qPCR. *, $p < 0.05$ (paired Student's *t* test).

RESULTS

Identification of Arl5B—To understand the contribution of Arl family members to RLR signaling, we employed expression screening. We co-transfected HEK293 cells with a series of expression plasmids for individual Arl family members and MDA5 together with a luciferase reporter plasmid driven by the IFNβ promoter (Fig. 1, *A* and *B*). Among the 18 Arl members tested, Arl5B overexpression was found to significantly decrease MDA5-induced luciferase expression. Arl5B has a GTP binding site and GTPase activating protein/guanine nucleotide exchange factor interaction site (Fig. 1*C*), and expression of Arl5B mRNA was up-regulated by poly(I:C) stimulation in MEFs as measured by qPCR analysis (Fig. 1*D*).

We then co-overexpressed MDA5 and different amounts of Arl5B in HEK293 cells and found that MDA5-mediated activation of the IFNβ promoter was suppressed by Arl5B in a dose-dependent manner (Fig. 2*A*). The suppressive effects of Arl5B on MDA5 were also found in poly(I:C)-stimulated conditions (Fig. 2*A*). In contrast, Arl5B overexpression failed to suppress RIG-I-mediated activation of an IFNβ promoter either in unstimulated cells or in cells stimulated with low molecular weight poly(I:C) (short poly(I:C); a RIG-I agonist) (Fig. 2*A*). MDA5-mediated NFκB activation was also suppressed by Arl5B overexpression in a reporter assay (Fig. 2*B*). Arl5B repressed the activation of an IFNβ promoter induced by full-length MDA5 but did not repress a deletion mutant of MDA5 encoding CARDs (Fig. 2*C*). Furthermore, Arl5B overexpression did not affect the IFNβ promoter activation induced by TRIF, TBK1, or IPS-1, signaling molecules that act downstream of RLRs (Fig. 2*D*). Arl5B has a GTP- or GDP-bound form that correlates with its function (32). We, therefore, investigated whether GTP/GDP binding to Arl5B affects Arl5B-mediated negative regulation of MDA5 using the expression plasmids of Arl5B Q70L and T30N, which cannot bind GDP and GTP, respectively. However, both Arl5B Q70L and T30N repressed MDA5-mediated activation of an IFNβ promoter to the same extent as wild type Arl5B (Fig. 2, *E* and *F*). These data suggest that Arl5B targets MDA5 or a molecule(s) upstream of MDA5 for the inhibition of type I IFN induction irrespective of its GTP/GDP binding.

Arl5B Knockdown Enhances MDA5 Signaling—We investigated the contribution of Arl5B to MDA5 signaling by shRNA-mediated knockdown in MEFs. We prepared three distinct shRNAs targeting the Arl5b gene and confirmed by qPCR analysis that all three suppressed Arl5b expression (Fig. 3*A*). We used two shRNAs (#1 and #2) due to their higher efficiency than #3 and found that mRNA expression of *Ifnb1*, *Ifna*, *Il6*, and *Tnf* in response to poly(I:C) stimulation was significantly enhanced in Arl5b-knockdown cells relative to Scramble shRNA-treated cells (Fig. 3*B*). In contrast, expression of these genes after stimulation with short poly(I:C) or lipopolysaccharide (LPS; a TLR4 agonist) was comparable between control and Arl5b-knockdown cells (Fig. 3*B*). Arl5b-knockdown cells exhibited enhanced IL-6 and CXCL10 production after poly(I:C) stimulation as measured by ELISA (Fig. 3*C*). Taken together, these findings suggest that Arl5B specifically suppresses MDA5-mediated responses.

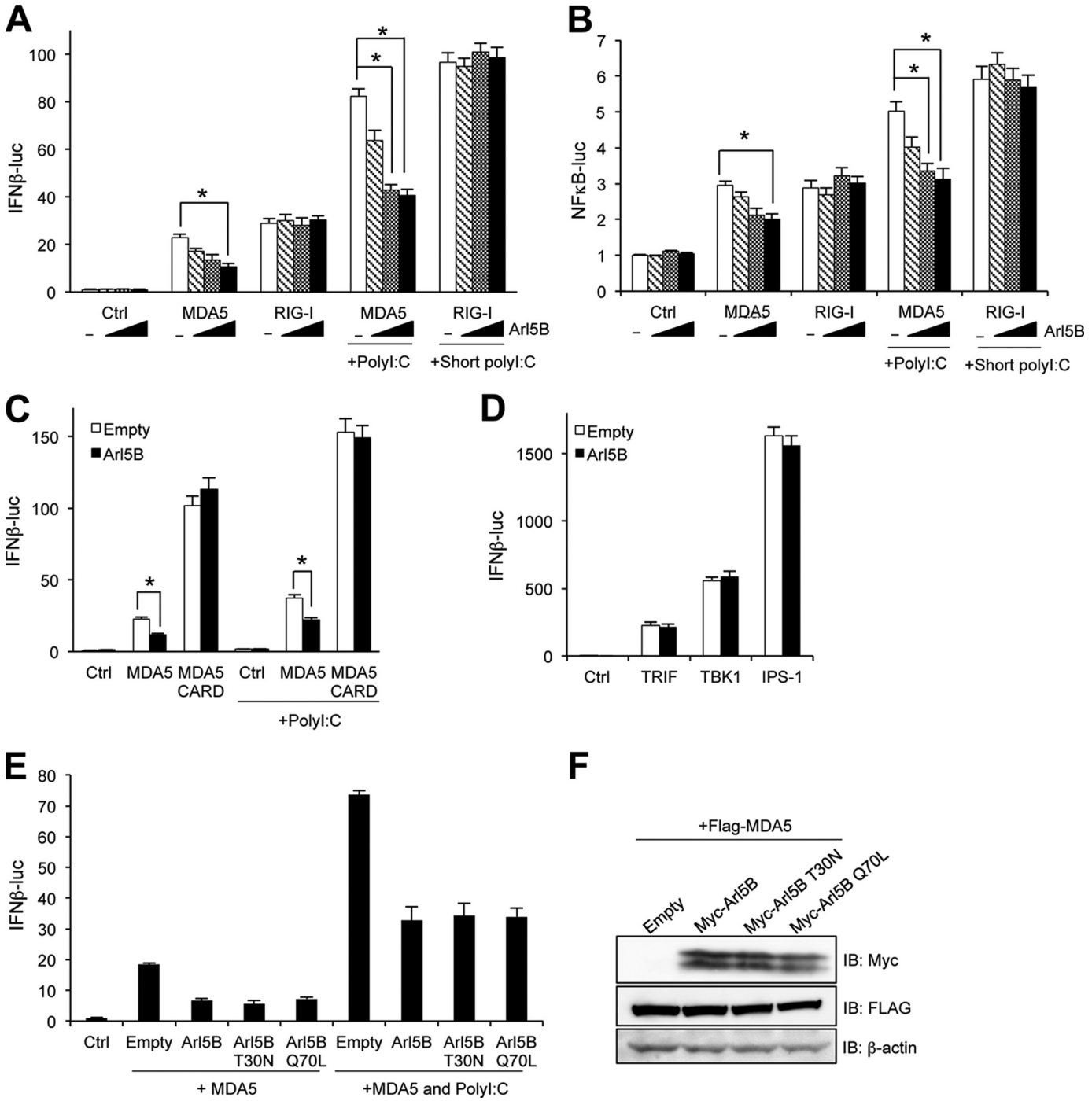

FIGURE 2. **Arl5B negatively regulates MDA5 but not RIG-I signaling.** *A* and *B*, HEK293 cells were transiently transfected with 0, 125, 250, or 500 ng of Arl5B expression plasmids (*white*, *striped*, *gray*, and *black bars*, respectively) and 100 ng of MDA5 or RIG-I expression plasmids together with an IFNβ (*A*) or NFκB (*B*) promoter-driven luciferase reporter plasmid. The cells were then stimulated with 1 μg/ml poly(I:C) or low molecular weight poly(I:C) (*short poly(I:C)*) for 24 h, after which luciferase activity was measured. *C*, HEK293 cells were transiently transfected with 500 ng of Arl5B and 100 ng of MDA5 or MDA5 CARD expression plasmids together with an IFNβ reporter plasmid. The cells were stimulated as in *A*, and luciferase activity was measured. *D* and *E*, HEK293 cells were transiently transfected with the indicated expression plasmids. Luciferase activity was measured ($n = 4$; mean values and S.E. are depicted). *F*, cell lysates prepared from HEK293 cells transiently transfected with the indicated plasmids were subjected to immunoblotting with the indicated antibodies. *, $p < 0.05$ (paired Student's *t* test).

Arl5B Interacts with MDA5—We tested interactions between MDA5 and Arl5B by co-immunoprecipitation assay using cell lysates prepared from HEK293T cells overexpressing Myc-tagged Arl5B along with FLAG-tagged MDA5 or RIG-I. Immunoblot analysis using anti-FLAG antibody revealed that FLAG-MDA5, but not FLAG-RIG-I, co-precipitated with Myc-Arl5B, indicating that Arl5B interacts with MDA5 but not with RIG-I (Fig. 4*A*). Next, we investigated which region of MDA5 is responsible for binding to Arl5B. To do so, we constructed deletion mutants of MDA5 encoding the N-terminal CARDs, the central RNA helicase domain, and the C-terminal domain. A co-immunoprecipitation assay indicated that Arl5B associated

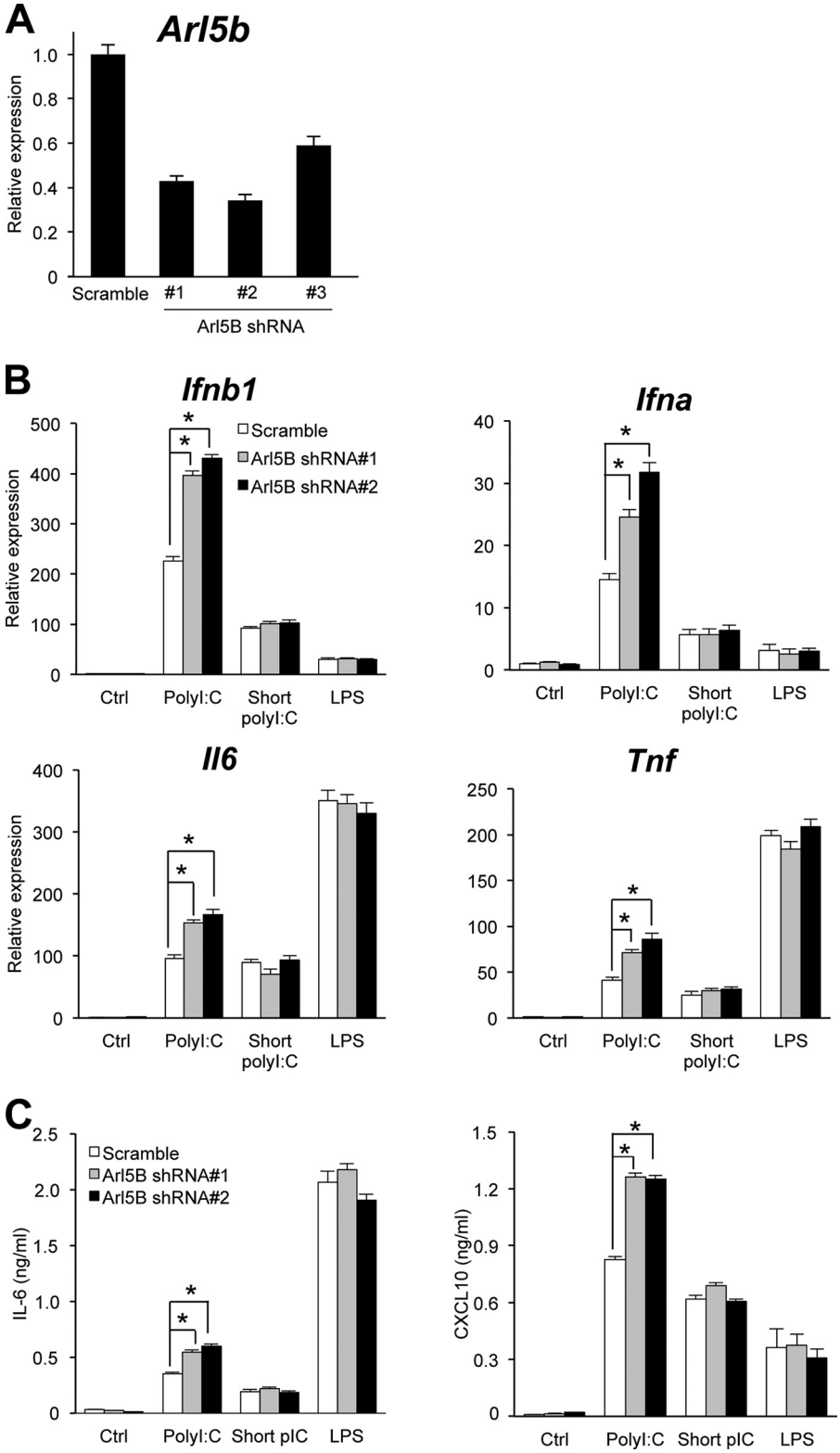

FIGURE 3. **Arl5B knockdown enhances MDA5 signaling.** *A*, MEFs were infected with Arl5B shRNA-expressing retrovirus. After puromycin selection of the MEFs, the efficiency of Arl5b knockdown was examined by qPCR. *B*, Scramble or Arl5B shRNA-expressed MEFs were stimulated with 1 μg/ml poly(I:C), short poly(I:C), or LPS for 8 h, and target gene expression was then measured by qPCR. *C*, Scramble or Arl5B shRNA-expressed MEFs were stimulated with 1 μg/ml poly(I:C), short poly(I:C), or LPS for 24 h, and the concentration of IL-6 and CXCL10 in the supernatant was measured by ELISA ($n = 3$; mean values and S.E. are depicted). *, $p < 0.05$ (paired Student's *t* test).

with the C-terminal domain but not with either the CARDs or the RNA helicase domain of MDA5 (Fig. 4*B*). Furthermore, FLAG-MDA5 was co-precipitated with anti-Arl5B antibody in HEK293T cells, indicating that endogenous Arl5B interacts with overexpressed FLAG-MDA5 (Fig. 4*C*). We then examined the intracellular localization of Arl5B and MDA5 by immuno-

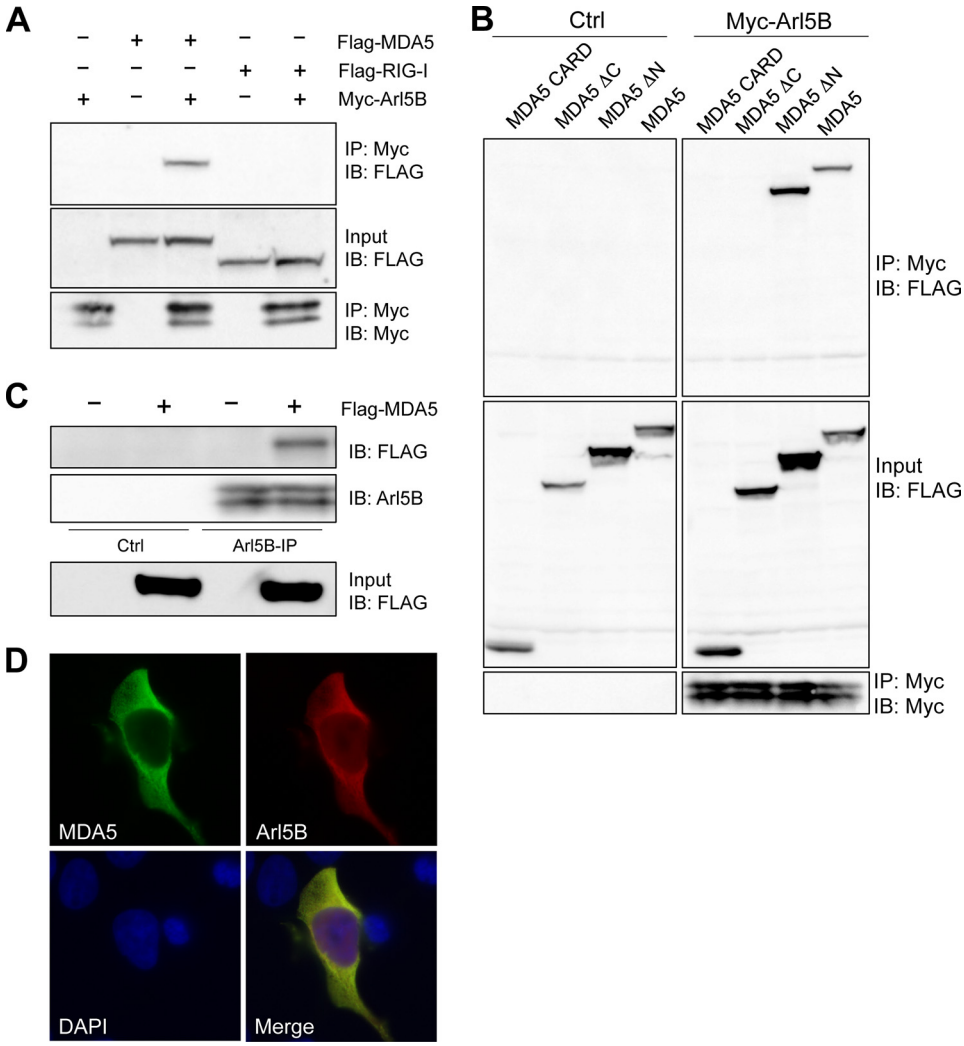

FIGURE 4. **Arl5B interacts with MDA5.** *A* and *B*, HEK293T cells were transiently transfected with Myc-Arl5B and either FLAG-MDA5 or FLAG-RIG-I (*A*) or transfected with Myc-Arl5B and either FLAG-MDA5, FLAG-MDA5 CARD (1–203), FLAG-MDA5 ΔC (1–575), or FLAG-MDA5 ΔN (204–1025) (*B*). The cell lysates were immunoprecipitated (*IP*) and blotted (*IP*) with the indicated antibodies. *C*, HEK293T cells were transiently transfected with FLAG-MDA5, and the cell lysates were immunoprecipitated using anti-Arl5B antibody and blotted with the indicated antibodies. *D*, HEK293T cells transiently transfected with Myc-Arl5B and FLAG-MDA5 were fixed and stained with Hoechst 33342 (*blue*), anti-Myc (*red*), or anti-FLAG (*green*) antibody. Data are representative of two independent experiments.

fluorescence. We overexpressed FLAG-MDA5 and Myc-Arl5B in HEK293 cells and visualized them by immunostaining. MDA5 exhibited cytoplasmic localization with a diffuse pattern (Fig. 4*D*); Arl5B also showed a localization similar to that of MDA5 (Fig. 4*D*). This finding suggests that Arl5B and MDA5 interact in the cytoplasm.

Enhanced MDA5-mediated Cytokine Production in Arl5B-deficient Cells—To further investigate Arl5B function in relation to MDA5 signaling *in vivo*, we generated Arl5B-deficient mice. No Arl5B-deficient mice were born after crossing heterozygous mice, suggesting that they are embryonic-lethal. No embryos were found after embryonic day 11.5 (Table 2). Therefore, we prepared fibroblast cells from wild type and Arl5B-deficient embryos at 9.5 days and used them for further analyses. Targeted disruption of the Arl5B locus in these MEFs and murine embryonic stem cells (ES cells) was confirmed by Southern blot and PCR analyses (Fig. 5, *A*, *B*, and *C*), and impaired Arl5B expression was checked by immunoblot (Fig. 5*D*).

Initially, we stimulated wild type and Arl5B-deficient cells with poly(I:C), short poly(I:C), or LPS and examined cytokine

TABLE 2

Genotyping of fetuses at different embryonic stages

Arl5b$^{+/-}$ male and Arl5b$^{+/-}$ female mice were mated, and the number of fetuses of each genotype was counted. The fetuses were obtained from three pregnant mice each group.

Embryonic day	Number of fetusus		
	Arl5B$^{+/+}$	*Arl5B*$^{+/-}$	*Arl5B*$^{-/-}$
9.5	7	16	8
11.5	9	18	2
13.5	8	17	0
15.5	8	15	0

mRNA expression by qPCR. Arl5B-deficient MEFs displayed enhanced expression of *Ifnb1*, *Ifna*, *Il6*, and *Tnf* after poly(I:C) stimulation compared with wild type cells, whereas the expression of these genes after stimulation with short poly(I:C) or LPS was comparable between wild and Arl5B-deficient MEFs (Fig. 6*A*). Arl5B-deficient cells exhibited enhanced IL-6 and CXCL10 production after poly(I:C) stimulation as measured by ELISA (Fig. 6*B*).

We then evaluated the responses of Arl5B-deficient MEFs to virus infection. We measured *Ifnb1* and *Il6* mRNA expression

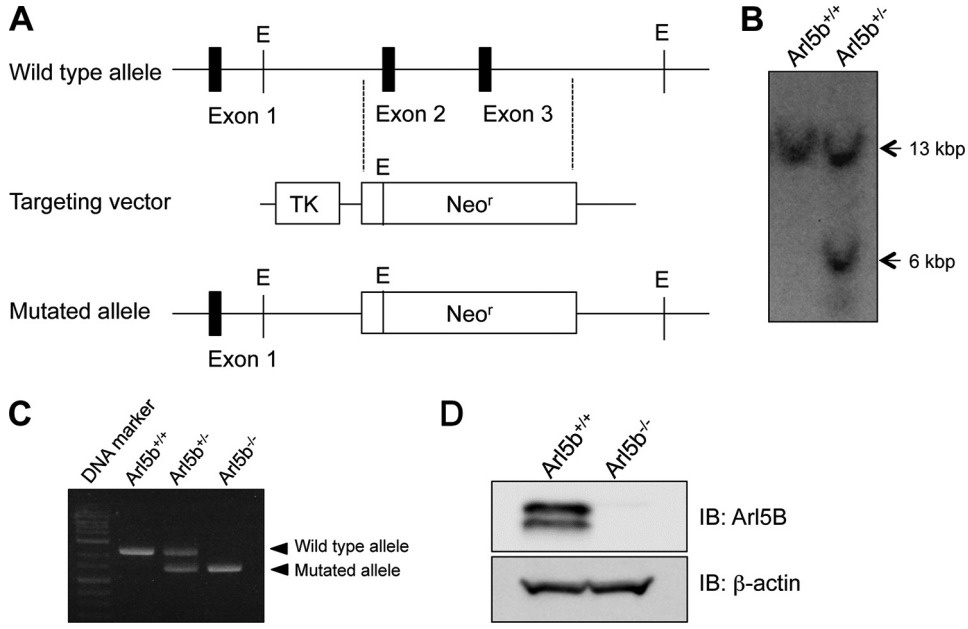

FIGURE 5. **Targeted disruption of Arl5b gene.** *A*, schematic representation of Arl5b locus disruption in murine genomic DNA. *E*, endonuclease sites. *B*, Southern blotting of wild type and Arl5b-heterozygous ES cells. *C*, genotyping of wild type and Arl5B-deficient MEFs by PCR. *D*, immunoblot (*IB*) analysis of Arl5B expression in wild type and Arl5B-deficient MEFs.

in cells infected with EMCV or NDV, which are known to be recognized by MDA5 or RIG-I, respectively. EMCV-induced *Ifnb1* and *Il6* expression were up-regulated about 1.7- and 2-fold, respectively, in Arl5B-deficient MEFs at 12 h post-infection (multiplicity of infection = 5). In contrast, expression of these genes after NDV infection was comparable between wild type and Arl5B-deficient MEFs (Fig. 6, *C* and *D*).

Next, we examined IRF3 and NFκB activation after poly(I:C) and short poly(I:C) stimulation by immunoblot. Phosphorylation of IRF3 Ser-396 and NFκB p65 Ser-536 was up-regulated in poly(I:C)-stimulated Arl5B-deficient MEFs compared with wild type MEFs (Fig. 6, *E* and *F*). By contrast, no such difference was found in the phosphorylation levels of IRF3 and NFκB in short poly(I:C)-stimulated cells (Fig. 6, *E* and *F*). These results suggest that Arl5B negatively regulates MDA5 signaling.

Arl5B Interferes with MDA5-dsRNA Interaction—Although Arl5A shares a high degree of sequence similarity with Arl5B (79% amino acid identity), it was unable to repress MDA5-dependent IFNβ promoter activation (Fig. 1*A*). We compared the amino acid sequences of both proteins and found that four regions display dissimilar amino acid sequences. To examine whether or not these regions in Arl5B are involved in the repression of MDA5-mediated responses, we generated four expression constructs for Arl5B, designated D1-D4, each lacking one of these regions (Fig. 7, *A* and *B*), and tested their ability to interact with MDA5 and suppress MDA5-mediated responses. A co-immunoprecipitation assay indicated that FLAG-MDA5 co-precipitated with full-length Myc-Arl5B, D2, D3, and D4, but not with D1, strongly suggesting that region 1 is necessary for binding to MDA5 (Fig. 7*C*). In agreement with this binding property, overexpression of Arl5B D2, D3, and D4, but not D1, repressed MDA5-mediated activation of an IFNβ promoter to a similar extent as full-length Arl5B in HEK293 cells (Fig. 7*D*). We next restored Arl5B expression in Arl5B-deficient MEFs using a retroviral expression system. Retrovirus-mediated transduction of Arl5B decreased the MDA5-mediated responses in Arl5B-deficient cells to a level similar to that seen in wild type cells (Fig. 7*E*). By contrast, the suppressive effect of Arl5B on MDA5 was not observed in Arl5B D1-transduced Arl5B-deficient MEFs (Fig. 7*E*). Because it was recently shown that MDA5 forms a filament along with RNA that is required for activation of downstream molecules (9, 11), we examined whether or not Arl5B disturbs the interaction between MDA5 and RNA. We transfected HEK293T cells with FLAG-MDA5 and either Myc-Arl5B or Myc-Arl5B D1, immunoprecipitated cell lysates with poly(I:C)-conjugated beads, and blotted with anti-FLAG antibody. FLAG-MDA5 precipitated with poly(I:C) beads, and this association was suppressed by overexpression of full-length Arl5B but not of Arl5B D1 (Fig. 7*F*). Taken together, these results suggest that region 1 of Arl5B is responsible for binding with MDA5 and for Arl5B-mediated inhibition of the MDA5-dsRNA interaction.

DISCUSSION

In this study we identified Arl5B as a negative regulator of MDA5. We found that Arl5B has the unique property of binding to MDA5 but not to RIG-I and inhibits MDA5-triggered antiviral innate immune responses. Currently, the kinase DAK is known as a negative regulator of MDA5. However, it is likely that DAK-mediated negative regulation of MDA5 differs from that mediated by Arl5B. DAK binds to MDA5 CARDs and thus to suppress MDA5-mediated activation of IRF3, suggesting that DAK inhibits the formation of a signalosome containing MDA5, IPS-1, TRAF3, TBK1/IKKi, and IRF3. By contrast, our data indicate that Arl5B binds to the CTD of MDA5 and suppresses both IRF3 and NFκB activation. Furthermore, overexpression of Arl5B decreased the interactions between MDA5 and poly(I:C) (Fig. 7*F*) but unaffected the interactions between

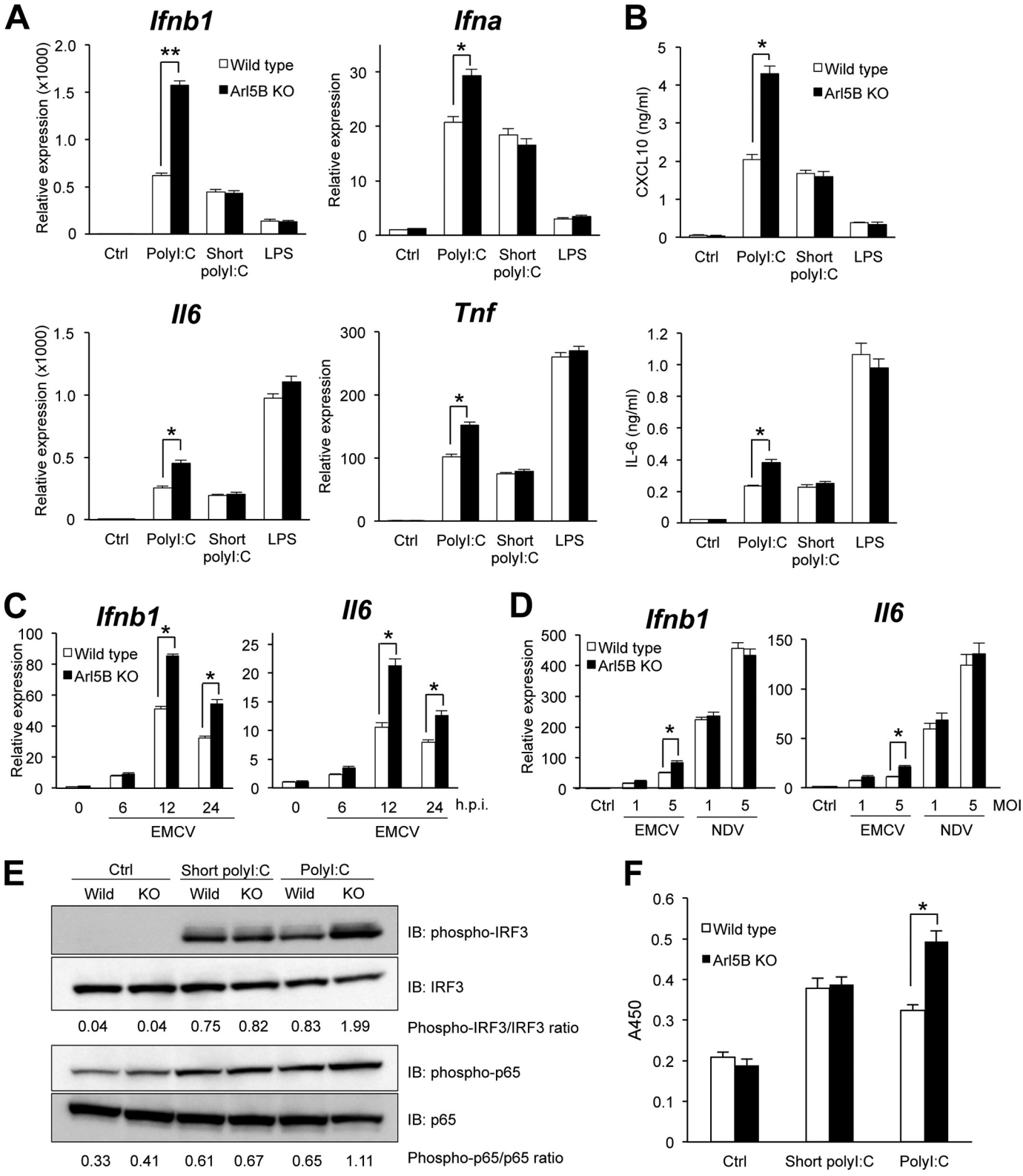

FIGURE 6. **MDA5-mediated signaling is up-regulated in Arl5B-deficient MEFs.** *A*, wild type and Arl5B-deficient (*KO*) MEFs were stimulated with 1 μg/ml poly(I:C), short poly(I:C), or LPS for 8 h, and expression of the indicated genes was measured by qPCR. *B*, MEFs were stimulated with 1 μg/ml poly(I:C), short poly(I:C), or LPS for 24 h, and cytokine concentration was measured by ELISA. *C*, MEFs were infected with EMCV at a multiplicity of infection of 5, and expression of the indicated genes was measured by qPCR at 6, 12, or 24 h post infection (*h.p.i.*). *D*, MEFs were infected with EMCV and NDV for 12 h at multiplicity of infection (*MOI*) of 1 or 5. Expression of the indicated genes was measured by qPCR. *E*, MEFs were stimulated with 1 μg/ml poly(I:C) or short poly(I:C) for 4 h, and cell lysates were blotted (*IB*) with the indicated antibodies. The indicated ratios of phospho-IRF3/IRF3 and phospho-NFκB p65/NFκB p65 were calculated from the band intensities using ImageJ software. *F*, wild type and Arl5B-deficinet MEFs were stimulated with 1 μg/ml short poly(I:C) or poly(I:C) for 4 h. DNA binding activity of NF-κB in the nuclear extracts were then evaluated by measuring absorbance at 450 nm with NF-κB probe DNA-based ELISA. $n = 3$; mean values and S.E. are depicted. *, $p < 0.05$; **, $p < 0.01$ (paired Student's *t* test).

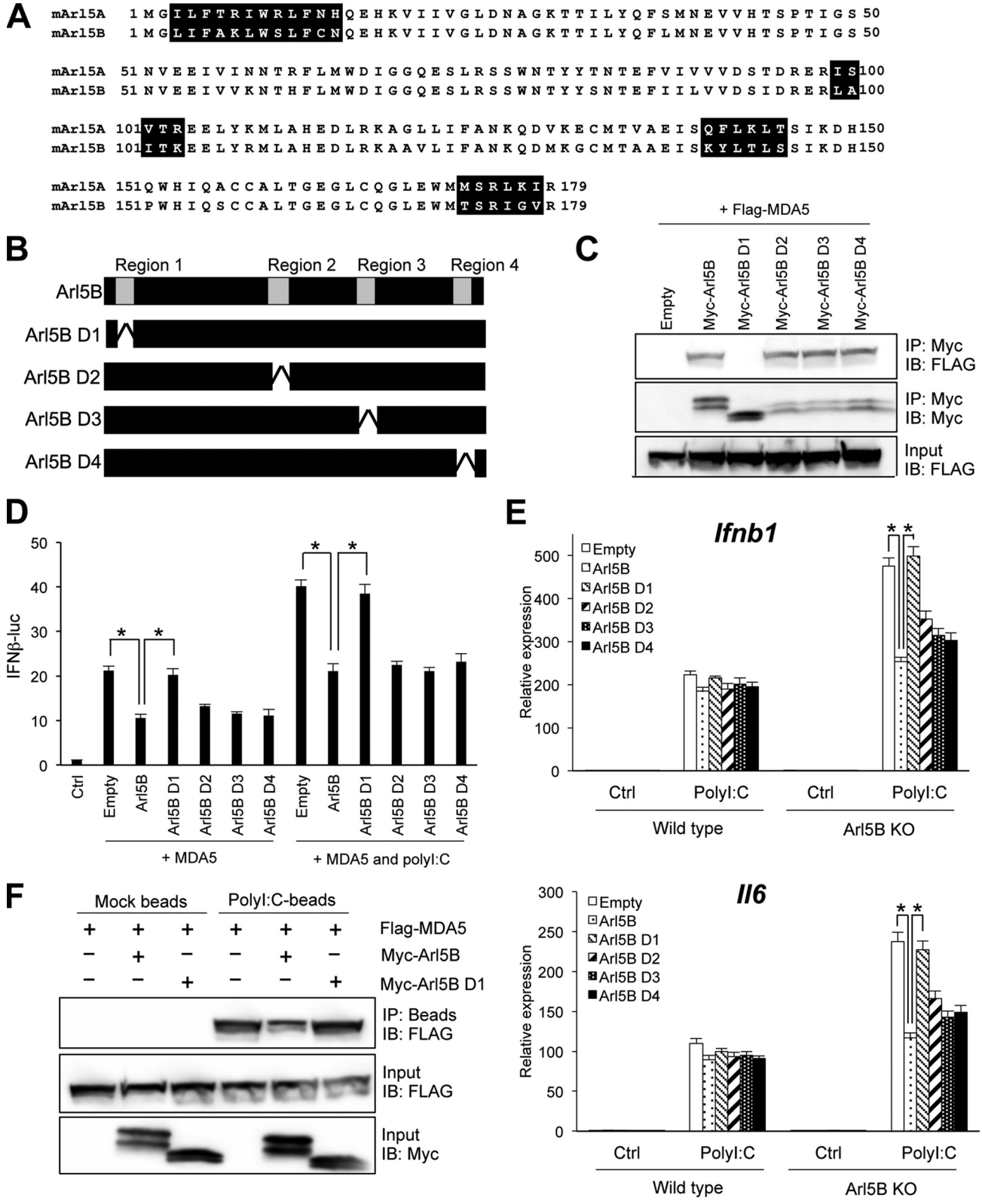

FIGURE 7. **MDA5-dsRNA association is disrupted by the Arl5B.** *A*, alignment of the amino acid sequences of Arl5A and Arl5B. Low similarity regions are indicated as *black boxes*. *B*, schematic representation of deletion mutants of Arl5B. *C*, HEK293T cells transiently co-transfected with FLAG-MDA5 and four Myc-tagged Arl5B mutants. The cell lysates were immunoprecipitated (*IP*) and blotted (*IB*) with the indicated antibodies. *D*, HEK293 cells transiently transfected with MDA5 and four Arl5B mutant expression plasmids were stimulated with or without 1 μg/ml poly(I:C), and luciferase activity was measured. *E*, wild type and Arl5B-deficient MEFs were infected with various Arl5B-expressing retroviruses. After puromycin selection, the cells were stimulated with 1 μg/ml poly(I:C) for 8 h, and *Ifnb1* and *Il6* expression was then measured by qPCR. *F*, Arl5B interferes with the binding of MDA5 with dsRNA via its N-terminal region. After transfection of HEK293 cells with MDA5 and Arl5B expression plasmids, cell lysates were precipitated with poly(I:C)-conjugated agarose beads and then immunoblotted with the indicated antibodies ($n = 3$; mean values and S.E. are depicted). *, $p < 0.05$ (paired Student's *t* test).

MDA5 and IPS-1 (data not shown). It has been shown that the MDA5 CTD is required for cooperative assembly of MDA5 on RNA, which enhances MDA5-mediated IPS-1 activation (9). Thus, Arl5B-mediated inhibition of MDA5 signaling is probably attributable to interference with MDA5 recognition of RNA.

MDA5 activation is regulated by multiple mechanisms, including posttranscriptional modification and intracellular localization (33, 34). MDA5 CARD is dephosphorylated by PP1 following virus infection and interacts with IPS-1 (33). However, our results demonstrate that Arl5B overexpression suppresses IFNβ promoter activation induced by the MDA5 S88A mutant, in which a phosphorylation site was disrupted (data not shown), suggesting that Arl5B inhibits MDA5 signaling via mechanisms that are distinct from PP1-mediated dephosphorylation. In addition to phosphorylation, the CARDs of MDA5 are known to associate with unanchored polyubiquitin chains, which facilitate the activation of downstream signaling in a manner that is analogous to the action of RIG-I (35). However, our finding that Arl5B interacts with the CTD of MDA5 and interferes with MDA5 recognition of RNA suggests that Arl5B suppresses MDA5 activation before ubiquitination.

The effect of Arl5B deficiency and overexpression on NFκB activation was small compared with IRF3 activation, suggesting that Arl5B preferentially suppresses IRF3 activation, although MDA5 signaling culminates in the activation of both IRF3 and NFκB. Currently, ATG16L1, TANK, CYLD, A20, and NLRX1 are known as negative regulators for NFκB activation in RLR, Toll-like receptor, and TNF receptor signaling (14). It may be possible that these molecules also negatively regulate MDA5-mediated NFκB activation and compensate the function of Arl5B at least in MEFs. Alternatively, Arl5B may play a major role in cells other than MEFs such as dendritic cells, which are the major sources of type I IFN upon virus infection. We, therefore, need to generate conditional knock-out mice in which Arl5B is deleted in these cells and understand cell type-specific roles of Arl5B in regulation of MDA5.

The subcellular localization of RLRs may also be a mechanism to regulate signaling. RIG-I and MDA5 translocate from the cytoplasm to the anti-viral stress granule, where viral and host RNAs are located (34, 36). Although the formation of this granule is arguably important for RNA recognition and initiation of downstream signaling, several reports imply that stress granule formation is dispensable for MDA5 activation (34, 37). In our experiments, stress granule formation in Arl5B-deficient MEFs treated with poly(I:C) was induced to an extent similar to that in wild type cells (data not shown). Moreover, intracellular trafficking of poly(I:C) into endosome was unaltered in wild and Arl5B-deficient MEFs as visualized using rhodamine-conjugated poly(I:C) (data not shown). These results suggest that Arl5B does not prevent the trafficking of MDA5 to stress granules and poly(I:C) incorporation.

The Arl family members are involved in multiple cellular processes, including endocytosis, Golgi-mediated transport, microtubule formation, and spermatogenesis (27). Previous studies showed that Arl5B translocates to the Golgi from the cytosol when it binds GTP and regulates retrograde membrane transport from the endosome to the trans-Golgi (32). However, the GTP binding-defective T30N mutant of Arl5B also had the capacity to suppress MDA5-mediated IFNβ promoter activity to the same degree as wild type Arl5B (Fig. 2*E*). Furthermore, we identified a region of Arl5B that was responsible for binding to MDA5 and that was distinct from the GTP binding site (Fig. 7*A*) (27). Therefore, Arl5B-mediated repression of MDA5 signaling is independent of GTP binding. Currently, the physiological role of GTP binding by Arl5B in terms of innate immune regulation remains unclear. However, given that the Arl5B-deficient mice that we generated exhibited embryonic lethality (Table 2), the GTP binding property of Arl5B may be involved in the regulation of development. It has been reported that Arl1 regulates AP-1 recruitment to the Golgi and secretory granule formation, and Arl1 mutation is lethal in *Drosophila* (38). Arl5B may also have a role in Golgi-mediated intercellular signaling that is important for proper embryo development. Other target molecules regulated by Arl5B should be investigated in future work to illuminate this point.

MS is a chronic inflammatory and demyelinating disease of the central nervous system that causes neuronal degeneration and axonal loss in the brain and spinal cord (39). Because inflammation is considered to be one of the driving forces of MS, many therapeutic approaches have been designed to target the inflammatory process (40, 41). Notably, Arl5B is highly expressed in the peripheral blood cells of MS patients and is induced by IFNβ treatment (29), implying a link between MS and Arl5B. Furthermore, gain-of-function mutations in MDA5 increase the risk for MS and autoimmune disease (15, 16, 18). We, therefore, speculate that Arl5B deficiency may lead to constitutive activation of MDA5 signaling and cause inflammatory symptoms. This could be tested by generating Alr5B conditional knock-out mice or mice that have a deletion in the N-terminal MDA5-interacting domain of Arl5B. Finally, it would be interesting to determine whether synthetic peptides derived from the N-terminal Arl5B, which could inhibit MDA5 activation, would reduce pathogenesis of MS or of any other autoimmune diseases in which MDA5 may be involved.

Acknowledgments—We thank S. Tarty for technical assistance, M. Takahama and T. Kondo for helpful discussions, and E. Kamada, M. Kageyama, A. Fujita, and K. Abe for secretarial assistance.

REFERENCES

1. Loo, Y. M., and Gale, M. Jr. (2011) Immune signaling by RIG-I-like receptors. *Immunity* **34,** 680–692
2. Yoo, J. S., Kato, H., and Fujita, T. (2014) Sensing viral invasion by RIG-I like receptors. *Curr. Opin. Microbiol.* **20,** 131–138
3. Kawai, T., and Akira S. (2006) Innate immune recognition of viral infection. *Nat. Immunol.* **7,** 131–137
4. Arnoult, D., Soares, F., Tattoli, I., and Girardin, S. E. (2011) Mitochondria in innate immunity. *EMBO Rep.* **12,** 901–910
5. Gack, M. U., Shin, Y. C., Joo, C. H., Urano, T., Liang, C., Sun, L., Takeuchi, O., Akira, S., Chen, Z., Inoue, S., and Jung, J. U. (2007) TRIM25 RING-finger E3 ubiquitin ligase is essential for RIG-I-mediated antiviral activity. *Nature* **446,** 916–920
6. Oshiumi, H., Miyashita, M., Inoue, N., Okabe, M., Matsumoto, M., and Seya, T. (2010) The ubiquitin ligase Riplet is essential for RIG-I-dependent innate immune responses to RNA virus infection. *Cell Host Microbe* **8,** 496–509
7. Zeng, W., Sun, L., Jiang, X., Chen, X., Hou, F., Adhikari, A., Xu, M., and Chen, Z. J. (2010) Reconstitution of the RIG-I pathway reveals a signaling

role of unanchored polyubiquitin chains in innate immunity. *Cell* **141,** 315–330
8. Kuniyoshi, K., Takeuchi, O., Pandey, S., Satoh, T., Iwasaki, H., Akira, S., and Kawai, T. (2014) Pivotal role of RNA-binding E3 ubiquitin ligase MEX3C in RIG-I-mediated antiviral innate immunity. *Proc. Natl. Acad. Sci. U.S.A.* **111,** 5646–5651
9. Peisley, A., Lin, C., Wu, B., Orme-Johnson, M., Liu, M., Walz, T., and Hur, S. (2011) Cooperative assembly and dynamic disassembly of MDA5 filaments for viral dsRNA recognition. *Proc. Natl. Acad. Sci. U.S.A.* **108,** 21010–21015
10. Berke, I. C., Yu, X., Modis, Y., and Egelman, E. H. (2012) MDA5 assembles into a polar helical filament on dsRNA. *Proc. Natl. Acad. Sci. U.S.A.* **109,** 18437–18441
11. Wu, B., Peisley, A., Richards, C., Yao, H., Zeng, X., Lin, C., Chu, F., Walz, T., and Hur, S. (2013) Structural basis for dsRNA recognition, filament formation, and antiviral signal activation by MDA5. *Cell* **152,** 276–289
12. Jacobs, J. L., and Coyne, C. B. (2013) Mechanisms of MAVS regulation at the mitochondrial membrane. *J. Mol. Biol.* **425,** 5009–5019
13. Clark, K., Nanda, S., and Cohen, P. (2013) Molecular control of the NEMO family of ubiquitin-binding proteins. *Nat. Rev. Mol. Cell Biol.* **14,** 673–685
14. Kondo, T., Kawai, T., and Akira, S. (2012) Dissecting negative regulation of Toll-like receptor signaling. *Trends Immunol.* **33,** 449–458
15. Enevold, C., Oturai, A. B., Sørensen, P. S., Ryder, L. P., Koch-Henriksen, N., and Bendtzen, K. (2009) Multiple sclerosis and polymorphisms of innate pattern recognition receptors TLR1–10, NOD1–2, DDX58, and IFIH1. *J. Neuroimmunol.* **212,** 125–131
16. Rice, G. I, del Toro Duany, Y., Jenkinson, E. M., Forte, G. M., Anderson, B. H., Ariaudo, G., Bader-Meunier, B., Baildam, E. M., Battini, R., Beresford, M. W., Casarano, M., Chouchane, M., Cimaz, R., Collins, A. E., Cordeiro, N. J., Dale, R. C., Davidson, J. E., De Waele, L., Desguerre, I., Faivre, L., Fazzi, E., Isidor, B., Lagae, L., Latchman, A. R., Lebon, P., Li, C., Livingston, J. H., Lourenço, C. M., Mancardi, M. M., Masurel-Paulet, A., McInnes, I. B., Menezes, M. P., Mignot, C., O'Sullivan, J., Orcesi, S., Picco, P. P., Riva, E., Robinson, R. A., Rodriguez, D., Salvatici, E., Scott, C., Szybowska, M., Tolmie, J. L., Vanderver, A., Vanhulle, C., Vieira, J. P., Webb, K., Whitney, R. N., Williams, S. G., Wolfe, L. A., Zuberi, S. M., Hur, S., and Crow, Y. J. (2014) Gain-of-function mutations in IFIH1 cause a spectrum of human disease phenotypes associated with up-regulated type I interferon signaling. *Nat. Genet.* **46,** 503–509
17. Eckard, S. C., Rice, G. I., Fabre, A., Badens, C., Gray, E. E., Hartley, J. L., Crow, Y. J., and Stetson, D. B. (2014) The SKIV2L RNA exosome limits activation of the RIG-I-like receptors. *Nat. Immunol.* **15,** 839–845
18. Funabiki, M., Kato, H., Miyachi, Y., Toki, H., Motegi, H., Inoue, M., Minowa, O., Yoshida, A., Deguchi, K., Sato, H., Ito, S., Shiroishi, T., Takeyasu, K., Noda, T., and Fujita, T. (2014) Autoimmune disorders associated with gain of function of the intracellular sensor MDA5. *Immunity* **40,** 199–212
19. Diao, F., Li, S., Tian, Y., Zhang, M., Xu, L. G., Zhang, Y., Wang, R. P., Chen, D., Zhai, Z., Zhong, B., Tien, P., and Shu, H. B. (2007) Negative regulation of MDA5- but not RIG-I-mediated innate antiviral signaling by the dihydroxyacetone kinase. *Proc. Natl. Acad. Sci. U.S.A.* **104,** 11706–11711
20. Xu, L., Xiao, N., Liu, F., Ren, H., and Gu, J. (2009) Inhibition of RIG-I and MDA5-dependent antiviral response by gC1qR at mitochondria. *Proc. Natl. Acad. Sci. U.S.A.* **106,** 1530–1535
21. Yang, Y. K., Qu, H., Gao, D., Di, W., Chen, H. W., Guo, X., Zhai, Z. H., and Chen, D. Y. (2011) ARF-like protein 16 (ARL16) inhibits RIG-I by binding with its C-terminal domain in a GTP-dependent manner. *J. Biol. Chem.* **286,** 10568–10580
22. Lin, R., Yang, L., Nakhaei, P., Sun, Q., Sharif-Askari, E., Julkunen, I., and Hiscott, J. (2006) Negative regulation of the retinoic acid-inducible gene I-induced antiviral state by the ubiquitin-editing protein A20. *J. Biol. Chem.* **281,** 2095–2103
23. Moore, C. B., Bergstralh, D. T., Duncan, J. A., Lei, Y., Morrison, T. E., Zimmermann, A. G., Accavitti-Loper, M. A., Madden, V. J., Sun, L., Ye, Z., Lich, J. D., Heise, M. T., Chen, Z., and Ting, J. P. (2008) NLRX1 is a regulator of mitochondrial antiviral immunity. *Nature* **451,** 573–577
24. Arimoto, K., Takahashi, H., Hishiki, T., Konishi, H., Fujita, T., and Shimotohno, K. (2007) Negative regulation of the RIG-I signaling by the ubiquitin ligase RNF125. *Proc. Natl. Acad. Sci. U.S.A.* **104,** 7500–7505
25. Friedman, C. S., O'Donnell, M. A., Legarda-Addison, D., Ng, A., Cárdenas, W. B., Yount, J. S., Moran, T. M., Basler, C. F., Komuro, A., Horvath, C. M., Xavier, R., and Ting, A. T. (2008) The tumour suppressor CYLD is a negative regulator of RIG-I-mediated antiviral response. *EMBO Rep.* **9,** 930–936
26. Fan, Y., Mao, R., Yu, Y., Liu, S., Shi, Z., Cheng, J., Zhang, H., An, L., Zhao, Y., Xu, X., Chen, Z., Kogiso, M., Zhang, D., Zhang, H., Zhang, P., Jung, J. U., Li, X., Xu, G., and Yang, J. (2014) USP21 negatively regulates antiviral response by acting as a RIG-I deubiquitinase. *J. Exp. Med.* **211,** 313–328
27. Burd, C. G., Strochlic, T. I., and Gangi Setty, S. R. (2004) Arf-like GTPases: not so Arf-like after all. *Trends Cell Biol.* **14,** 687–694
28. Tuli, A., Thiery, J., James, A. M., Michelet, X., Sharma, M., Garg, S., Sanborn, K. B., Orange, J. S., Lieberman, J., and Brenner, M. B. (2013) Arf-like GTPase Arl8b regulates lytic granule polarization and natural killer cell-mediated cytotoxicity. *Mol. Biol. Cell.* **24,** 3721–3735
29. Boppana, S., Mindur, J. E., Balashov, K. E., Dhib-Jalbut, S., and Ito, K. (2013) Comparison of IFN-β inducible gene expression in primary-progressive and relapsing-remitting multiple sclerosis. *J. Neuroimmunol.* **265,** 68–74
30. Kato, H., Takeuchi, O., Sato, S., Yoneyama, M., Yamamoto, M., Matsui, K., Uematsu, S., Jung, A., Kawai, T., Ishii, K. J., Yamaguchi, O., Otsu, K., Tsujimura, T., Koh, C. S., Reis e Sousa, C., Matsuura, Y., Fujita, T., and Akira, S. (2006) Differential roles of MDA5 and RIG-I helicases in the recognition of RNA viruses. *Nature* **441,** 101–105
31. Walkiewicz, M. P., Basu, D., Jablonski, J. J., Geysen, H. M., and Engel, D. A. (2011) Novel inhibitor of influenza non-structural protein 1 blocks multicycle replication in an RNase L-dependent manner. *J. Gen. Virol.* **92,** 60–70
32. Houghton, F. J., Bellingham, S. A., Hill, A. F., Bourges, D., Ang, D. K., Gemetzis, T., Gasnereau, I., and Gleeson, P. A. (2012) Arl5b is a Golgi-localised small G protein involved in the regulation of retrograde transport. *Exp. Cell Res.* **318,** 464–477
33. Wies, E., Wang, M. K., Maharaj, N. P., Chen, K., Zhou, S., Finberg, R. W., and Gack, M. U. (2013) Dephosphorylation of the RNA sensors RIG-I and MDA5 by the phosphatase PP1 is essential for innate immune signaling. *Immunity* **38,** 437–449
34. Onomoto, K., Jogi, M., Yoo, J. S., Narita, R., Morimoto, S., Takemura, A., Sambhara, S., Kawaguchi, A., Osari, S., Nagata, K., Matsumiya, T., Namiki, H., Yoneyama, M., and Fujita, T. (2012) Critical role of an antiviral stress granule containing RIG-I and PKR in viral detection and innate immunity. *PLos ONE* **7,** e43031
35. Jiang, X., Kinch, L. N., Brautigam, C. A., Chen, X., Du, F., Grishin, N. V., and Chen, Z. J. (2012) Ubiquitin-induced oligomerization of the RNA sensors RIG-I and MDA5 activates antiviral innate immune response. *Immunity* **36,** 959–973
36. Lee, H., Komano, J., Saitoh, Y., Yamaoka, S., Kozaki, T., Misawa, T., Takahama, M., Satoh, T., Takeuchi, O., Yamamoto, N., Matsuura, Y., Saitoh, T., and Akira, S. (2013) Zinc finger antiviral protein mediates retinoic acid inducible gene I-like receptor-independent antiviral response to murine leukemia virus. *Proc. Natl. Acad. Sci. U.S.A.* **110,** 12379–12384
37. Okonski, K. M., and Samuel, C. E. (2013) Stress granule formation induced by measles virus is protein kinase PKR dependent and impaired by RNA adenosine deaminase ADAR1. *J. Virol.* **87,** 756–766
38. Torres, I. L., Rosa-Ferreira, C., and Munro, S. (2014) The Arf family G protein Arl1 is required for secretory granule biogenesis in *Drosophila*. *J. Cell Sci.* **127,** 2151–2160
39. Hauser, S. L., and Oksenberg, J. R. (2006) The neurobiology of multiple sclerosis: genes, inflammation, and neurodegeneration. *Neuron.* **52,** 61–76
40. Pfender, N., and Martin, R. (2014) Daclizumab (anti-CD25) in multiple sclerosis. *Exp Neurol.* **262PA,** 44–51
41. Brinkmann, V., Billich, A., Baumruker, T., Heining, P., Schmouder, R., Francis, G., Aradhye, S., and Burtin, P. (2010) Fingolimod (FTY720): discovery and development of an oral drug to treat multiple sclerosis. *Nat. Rev. Drug Discov.* **9,** 883–897